PAPER • **OPEN ACCESS**

Hydrogen as a direct heat exchange fluid in room temperature hydride systems: Numerical study on the desorption process

Journal of Physics: Conference Series **2893** (2024) 012081 doi:10.1088/1742-6596/2893/1/012081

Hydrogen as a direct heat exchange fluid in room temperature hydride systems: Numerical study on the desorption process

Ferdinando Vincenti[1], Gianluca Valenti[1,*]

Politecnico di Milano, Dipartimento di Energia, Via Lambruschini 4/a, 20156 Milano, ITALY

*gianluca.valenti@polimi.it

Abstract

Hydrogen, as an energy carrier, is a promising candidate to foster decarbonization. However, its storage poses significant challenges. Common methods, such as compressed gas and liquid hydrogen, have high energy consumption and safety concerns. Recently, solid hydrogen storage in materials like metal hydrides has gained attention for their ability to store hydrogen safely at low pressures and low temperatures. This study aims to develop a numerical model to simulate the performance of metal hydrides using hydrogen as a direct fluid heat exchanger during desorption. The model, formulated as a system of partial differential equations, is implemented in MATLAB with the ODE15s solver and applied to a disk-type lanthanum nickel reactor to minimize pressure drops. Performance is investigated by varying design parameters, including reactor length and diameter, bed porosity, hydride particle diameter, operating pressure and temperature, and hydrogen mass flow rate at the reactor inlet. Additionally, the energy consumption of auxiliary equipment, such as pumping and thermal power, is evaluated. Results show that the system energy requirement is about 8-9% of the hydrogen lower heating value, with most desorption occurring in less than 300 seconds. The reactor dimensions are crucial for fast desorption and low pressure drops, with pumping power under 1 W given the small thickness and flow rate. Particle diameter and porosity have minor impacts, while pressure, temperature, and flow rate are fundamental. High temperatures, low pressures, and high recirculating flow rates favor the reaction, though a trade-off between performance and energy consumption is necessary since all high temperatures high recirculated mass flow rate allows for high consumption.

Keywords: Hydrogen Storage, Metal Hydrides, Numerical Simulation, Direct heat exchanger

1 Introduction

The imperative for decarbonization grows more urgent each year. Governments worldwide are enacting laws to facilitate the energy transition. A primary challenge facing the scientific community in the decarbonization effort is the storage of energy, particularly renewable energy. Currently, there are no viable methods for large-scale storage of clean energy produced by renewables. Hydrogen is a promising candidate as a decarbonized energy vector that can advance decarbonization efforts and serve as a mean for energy storage [1].

The storage of hydrogen presents significant challenges that hinder its potential application. Common methods for hydrogen storage include compressed gas and liquid forms, both of which have high energy consumption and safety concerns. Recently, solid hydrogen storage in materials such as metal hydrides has gained attention due to their ability to store hydrogen safely at relatively low pressures and temperatures. By selecting appropriate compounds, it is possible to develop hydrides that work at room temperature and pressures as low as a few bars, achieving volumetric energy densities higher than that of liquid hydrogen. The absorption and desorption of hydrogen in hydrides are chemical reactions driven by thermal energy. Thus, effective thermal management of metal hydrides is crucial for optimizing their absorption and desorption performances. To ensure adequate surface area and energy density, hydrides are often pulverized. However, pulverized hydrides exhibit low thermal conductivity, making it challenging to efficiently supply heat to the hydride. The effort of the scientific research in this field is focused on developing more efficient thermal management arrangements to improve the performance of this technology.

Hydrides were initially discovered and studied in the 1970s and 1980s, predominantly within research laboratories in the United States [2], [3]. These early investigations laid the groundwork for

our contemporary comprehension of hydrides, delving into their properties, behaviors, and potential applications. The primary objective was to delineate the fundamental characteristics of hydride materials, subsequently facilitating more detailed explorations into their viability for energy storage and other applications. Building upon this foundation, various researchers have conducted analyses and reviews on the field [4], [5], [6]. These reviews have underscored pivotal aspects such as absorption and desorption kinetics, as well as the thermodynamic stability of hydrides. Such analyses have been instrumental in providing a deeper understanding of the physical phenomena and technological challenges associated with these systems. Numerical modeling has emerged as a significant tool in advancing our understanding of metal hydrides.

Numerous scientists have formulated models to simulate the behavior of different hydrides under varying conditions, employing different heat exchange management techniques [7], [8], [9]. Most of these studies have concentrated on modeling lanthanum nickel alloy, one of the most common hydrides. These models have been used to predict hydride system performance, optimizing their design, and elucidating the influence of various parameters on efficiency. Their development has facilitated more precise experimentation and provided valuable insights into the mechanisms governing hydride behavior. When applied to hydrogen storage, these models have highlighted the bottleneck hindering the adoption of metal hydrides, namely the efficient supply of heat. Nasrallah's study indicates a desorption time of approximately 12 minutes, while other studies have reported shorter durations depending on heat exchange arrangements and tank design, however all in the range of 5 to 10 minutes. In addition to numerical modeling, experimental and field studies have been conducted to validate these models and evaluate hydride performance in practical settings. Various heat exchange management techniques have been employed in these studies to assess their efficacy and enhance hydride performance [10].

These investigations have also identified potential implementation challenges and proposed strategies for overcoming them. Other authors have explored alternative heat exchange arrangements, including the use of foams and carbon nanotubes to enhance heat transfer within hydride materials [11], [12]. These enhancements aim to mitigate thermal conductivity issues associated with hydrides, thereby improving their efficiency and performance. Experimental studies incorporating such materials have shown promise, suggesting their potential significance in future hydride technology development. Chandra et al. developed a system utilizing heat pipes, significantly reducing desorption time from 2100 s to 900 s [13]. Lototskyy et al. in a series of work applied the technology to a series of vehicles proving that can they be effectively coupled with fuel cells. [14], [15]. One particularly promising strategy for addressing thermal management issues in hydride systems involves employing hydrogen as a direct contact heat exchange fluid. Recent numerical studies focusing on magnesium hydrides have demonstrated significant potential for this approach [16], [17]. These studies propose that utilizing hydrogen as a heat transfer medium can enhance heat exchange efficiency, consequently improving overall system performance. However, employing hydrogen as a direct heat exchange fluid poses challenges related to pressure drops within the reactor. To mitigate this, Yoshida et al. employed a sheet-type reactor where hydrogen flows between the sheets rather than through the media, while Song et al. observed high pumping power when hydrogen passed through the hydride.

When assessing hydrogen storage systems, relying solely on metrics such as released mass and release time overlooks other crucial factors that determine the viability of a technology. Considerations such as gravimetric and volumetric energy density, cost, cyclability, auxiliary consumptions, and safety significantly influence the attractiveness of a particular technology. Understanding how these key performance indicators interplay with system design is essential for comprehensively evaluating the potential of hydrides for hydrogen storage. The objective of this study is to develop a numerical model for simulating the performance of metal hydrides utilizing hydrogen as a direct fluid heat exchanger during the desorption process. The model is formulated as a system of partial differential equations and implemented in MATLAB using the ODE15s solver. Specifically, the model is applied to a case study involving a disk-type lanthanum nickel reactor to minimize pressure drops. The performance of the hydride is investigated by varying several design parameters,

including the reactor length and diameter, bed porosity, hydride particle diameter, operating pressure and temperature, and hydrogen mass flow rate at the reactor inlet. Additionally, evaluating the energy consumption of auxiliary equipment required to support heat exchange methods, such as pumping power and thermal power, is critical.

The novelty of this study lies in the unique heat exchange configuration proposed for room temperature hydrides and the consideration of auxiliary consumption, a topic that has not received attention in contemporary literature. By addressing these aspects, this research aims to contribute to a more thorough understanding of hydride-based hydrogen storage systems and pave the way for enhanced performance and efficiency in practical applications.

The paper is organized as follows. Chapter 2 describes the methods used to develop the numerical model for the investigations as well as the data used, and the case study selected. Chapter 3 presents the results of the study, and a discussion of these results. Chapter 4 provides the conclusions and offers final remarks on potential future work.

2 System description and model

This chapter addresses the analyzed system layout, the methodology used to develop the numerical model, and an overview of the case studies simulated with the numerical model to generate the results.

2.1 System layout

Figure 1 shows the layout of the system. A fan is employed to circulate the flow within the circuit, facilitating efficient heat transfer. A heat exchanger is integrated into the system to regulate the temperature of the hydrogen entering the metal hydride. During the endothermic desorption reaction, the heat exchanger provides hot hydrogen. This thermal management strategy ensures good conditions for the hydride reaction, improving performance and efficiency.

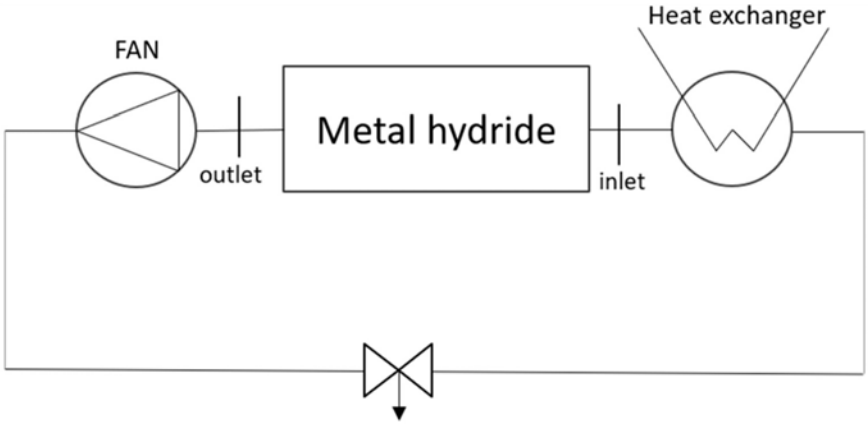

Figure 1: Simulated set-up with heat exchanger, metal hydride and fan.

2.2 Mathematical model

The mathematical model used to produce the results is based on the specific solution of the transport equations for energy, momentum and mass. The energy and mass equations are cast for both the solid and the gas phase while the equation for the momentum is related only to the gas phase. The basic formulation is taken from Mohammadashi et al. [8], however it is slightly modified to account for the different heat exchange mechanism that is employed in this specific case.
The basic form of the transport equations is:

Continuity Equation:
$$\frac{\partial \rho}{\partial t} + div(\rho \vec{u}) = 0 \quad (1)$$

x-momentum: $$\frac{\partial \rho u}{\partial t} + div(\rho u \vec{u}) = -\frac{\partial p}{\partial x} + div\big(\mu\ grad(u)\big) + S_{m_x} \quad (2)$$

y-momentum: $$\frac{\partial \rho v}{\partial t} + div(\rho v \vec{u}) = -\frac{\partial p}{\partial y} + div\big(\mu\ grad(v)\big) + S_{m_y} \quad (3)$$

z-momentum: $$\frac{\partial \rho w}{\partial t} + div(\rho w \vec{u}) = -\frac{\partial p}{\partial z} + div\big(\mu\ grad(w)\big) + S_{m_x} \quad (4)$$

Energy: $$\frac{\partial \rho i}{\partial t} + div(\rho i \vec{u}) = -p div(\vec{u}) + div\big(k\ grad(T)\big) + S_i + \phi \quad (5)$$

where ρ is the density, u is the vector of velocity, μ is the viscosity, i is the internal energy, k the thermal conductivity, S is the source term and ϕ is the dissipation term.

A series of assumptions is made to simplify the implementation of the system of transport equation:

- the phenomenon is 1-D dominated, only the dimension along direction x is considered,
- the effect of pressure in the energy balance is neglected,
- the effect of the viscous stresses in the momentum balance is neglected,
- the source term in the momentum balance is expressed with the Darcy law,
- given the pressure and temperature in play it is possible to use the ideal gas law for hydrogen,
- the reactor is adiabatic to external effects,
- efficiency of auxiliary components is neglected.

Considering the assumptions the expression of the equation of transport for the solid and the gas phase is:

energy balance on gas: $$\frac{\partial T_g}{\partial t} = \frac{\lambda_g}{\epsilon \rho_g c p_g}\frac{\partial^2 T_g}{\partial x^2} - \frac{v_x}{\epsilon}\frac{\partial T_g}{\partial x} + \frac{H_{gs}\big(T_g - T_s\big)A_{ex}}{\epsilon \rho_g c p_g} - \frac{T_g}{\epsilon}\frac{\partial v_x}{\partial x} \quad (6)$$

energy balance on solid: $$\frac{\partial T_s}{\partial t} = \frac{\lambda_s}{(1-\epsilon)\rho_s c p_s}\frac{\partial^2 T_s}{\partial x^2} - \frac{n\Delta H}{(1-\epsilon)\rho_s c p_s} + \frac{H_{gs}\big(T_g - T_s\big)A_{ex}}{(1-\epsilon)\rho_g c p_g} \quad (7)$$

mass balance on gas: $$\frac{\partial \rho_g}{\partial t} = -\frac{n}{\epsilon} - \frac{\partial \rho_g}{\partial x}\frac{v_x}{\epsilon} - \frac{\partial v_x}{\partial x}\frac{\rho_g}{\epsilon} \quad (8)$$

mass balance on solid: $$\frac{\partial \rho_s}{\partial t} = \frac{n}{1-\epsilon} \quad (9)$$

momentum balance: $$\frac{\partial v_g}{\partial t} = -v_x\frac{\partial v_x}{\partial x} - \frac{1}{\rho_g}\frac{\partial P}{\partial x} - \frac{\mu}{\epsilon \rho_g K_s}v_x \quad (10)$$

In the 1-D time variant transport equations some parameters are taken from literature and some other are computed using other auxiliary models. The constants that are taken from literature are the thermal conductivity of hydrogen and hydride (λ_s, λ_g), the enthalpy of reaction (ΔH) and the specific heat of gas and solid.

The other constants are computed with auxiliary models. The model for the chemical kinetics is usually based on a combination of analytical analysis fitted with experimental results. The chemical kinetics, n, is a function of concentration, temperature and pressure. The equation to compute n is taken from Mayer et al. [18] that was then used again by many other researchers. [19], [20], and can be expressed as:

$$n = C_d \times e^{-\frac{E_d}{R_g T_s}} \times \frac{P_g - P_{eq}}{P_g} \times \rho_s \tag{11}$$

where E_d and E_a are the activation energy for desorption and absorption and C_d and C_a are the kinetics constants. P_{eq} is the equilibrium pressure and ρ_{ss} is the density of the solid when is full of hydrogen. The expression of the equilibrium pressure, P_{eq}, is taken by Nasrallah et al. [19]**.** and is expressed as:

$$P_{eq} = f(wt) \times e^{-\frac{\Delta H}{R}\left(\frac{1}{T_s} - \frac{1}{T_{ref}}\right)} \tag{12}$$

where $f(wt)$ being a polynomial function of 7th grade for absorption and 9th grade for desorption of the amount of hydrogen inside the hydride. The amount of hydrogen inside the hydride is expressed with the atomic ratio H/M. $f(wt)$ can be expressed as:

$$f(wt) = \sum a_i * \left(\frac{H}{M}\right)^i \tag{13}$$

The values for the polynomial function are given in the input section of this work.

The value of the external surface of the hydride, fundamental to compute the heat exchanged between the gas and the solid phase, is taken from Logan et al and is computed as:

$$A_{ex} = \frac{6(1-\epsilon)}{d_p} \tag{14}$$

where ϵ is the porosity and d_p is the particle diameter [21].

The heat exchange coefficient, H_{gs}, is taken from a correlation developed in 2001 by Kuwahara et al. with the following expression:

$$H_{gs} = \frac{\lambda_g}{dp}\left(1 + \frac{4(1-\epsilon)}{\epsilon} + \frac{1}{2}(1-\epsilon)^{0.5} Re_{dp}^{0.6} Pr^{\frac{1}{3}}\right) \tag{15}$$

where λ_g is the hydrogen thermal conductivity, Pr is the Prandtl number and Re is the Reynolds number referred to the particle diameter [22]

The permeability of the metal hydride, K, to the passage of hydrogen is expressed with the Kozeny-Carman equation as:

$$K = \frac{1}{5}\frac{\epsilon^3}{1-\epsilon^2}\frac{1}{\left(\frac{6}{d_p}\right)^2} \tag{16}$$

To obtain the solution of the system of partial differential equations it is necessary to specify the initial and boundary conditions. The initial conditions are all known and are expressed as:

$$T_g(0,x) = T_{g,0} \qquad T_s(0,x) = T_{s,0} \qquad \rho_s(0,x) = \rho_{s,0}$$

$$P_g(0,x) = P_{g,0} \qquad \rho_g(0,x) = f(P_{g,0}, T_{g,0}) \qquad v_g(0,x) = 0$$

Dirichlet boundary conditions are used at the inlet of the reactor as a starting point. The inlet conditions of the reactor are all known. To perform the integration, it is decided to use the upwind differentiation scheme for the first order derivatives and the central differentiation scheme for the second order derivatives. The model is implemented in MATLAB using the ODE15s solver.

The model is utilized to conduct a series of simulations, wherein certain parameters are varied within predefined ranges. The investigated variables are the geometrical dimensions of the metal hydride, particle diameters, porosity, initial pressure, temperature, and mass flow rate. These variables are categorized into three distinct groups: geometry, porometry, and thermodynamics. Each simulation focuses on varying variables within one set while keeping the others constant. For instance, the

geometry and porometry parameters remain fixed while the thermodynamic variables are altered, and vice versa. This approach allows for a systematic exploration of the effects of individual parameters on the performance of the hydride system. The main performance indicator for this work other than the desorbed mass flow rate and the desorption time is the auxiliary consumption. The auxiliaries are the fan and the heat exchanger and to describe their behaviour both the power and the energy consumption are used with the following equations:

Pump power: $$P_p = \Delta P \times v_g \times S_t \quad (17)$$

Pump energy: $$E_p = \int_{t_{start}}^{t_{end}} P_P(t) \quad (18)$$

Thermal power: $$P_{th} = m_g \times c_{p,g} \times \Delta T \quad (19)$$

Thermal energy: $$E_{th} = \int_{t_{start}}^{t_{end}} P_{th}(t) \quad (20)$$

Where S_t is the cross section of the hydride and ΔP is the pressure drop across the hydride. For the purpose of this work the efficiencies of the machines are not considered.

2.3 Model input data

The variables analyzed parametrically in this work are the geometry of the hydride, length and diameter, the porosity of the hydride, i.e. the void fraction, the particles diameters and the thermodynamic variables such as pressure temperature and mass flow rate. Table 1 provides a list of all variables subjected to parametric analysis along with the corresponding range of values explored to generate the results. Meanwhile, Table 2 outlines the fixed input values utilized in the model for all simulations.

Table 1: Model variables that are changing between different simulations

Geometry	
Internal diameter [m]	0.06 – 0.14
Length of the hydride [m]	0.003 – 0.01
Porometry	
Particles Diameter [m]	50e-6 – 300e-6
Porosity [-]	0.4 – 0.6
Thermodynamics	
Temperature [K]	340 – 360
Pressure [Bar]	4 - 7
Flow rate [g/s]	0.05 - 0.1

The fixed inputs are related to the properties of hydrogen gas, properties of the metal hydride of choice and parameters for the numerical model.

Table 2*:* Fixed parameters of the model that does not change between different simulations

Variable [unit of measure]	Value
Hydride Molar mass [kg/mol]	0.43
Hydride empty density [kg/m^3]	8310
Maximum weight of hydrogen [%]	1.41
Enthalpy of reaction [J/molH2)]	30800
Entropy of reaction [J/(mol*k)]	108
Hydride specific heat [J/kg*K]	419
Hydride thermal conductivity [W/(m*k)]	1.04
Activation energy for desorption [J/mol]	16423
Kinetic constant for desorption [1/s]	9.57
Polynomial coefficients desorption reaction [-]	[0.420605 -4.11352 14.1799 -13.1085 4.55729 0.165833 -0.5923 0.178977 -0.023008 0.00112613]
Reference temperature [K]	300
Reference pressure [Bar]	1
Starting solid temperature [K]	300
Starting gas velocity [m/s]	0
Length of control volumes [m]	5.00E-05
relative tolerance ODE [-]	1.00E-06
Absolute tolerance ODE [-]	1.00E-06
Maximum timestep [s]	0.1

Other than the parametric analysis is presented a reference case used as a base to compare the results. Within the reference case the variables presented before are held constant at the average value of the fork presented in Table 1. The reference case is established with a hydride diameter of 0.08 m and a length of 0.005 m, a porosity of 0.5, a particle diameter of 100 microns, a gas inlet temperature of 350 K, thus a temperature difference given by the heat exchanger of 50 K, a pressure of 5 bar, and an inlet flow rate of 0.1 g/s.

3 Results and discussion

This section presents the results of the numerical model and discusses the findings. The performance of the metal hydrides is assessed using metrics such as desorption time, desorbed mass, and the consumption and power of the the fan and heat exchanger. Given that there are seven variables involved in the sensitivity analysis, numerous cases are generated. To provide a clear graphical representation of the results, a reference case is selected. The results of the reference case are presented at the beginning of Section 3. To show the results two of the three sets of variables are kept constant while the third is varied within the ranges presented in Table 1.

3.1 Reference case

Figure 2 shows the results for the reference case. Due to the small dimensions of the metal hydride, the desorption of hydrogen within occurs rapidly, taking less than 600 seconds. The total hydride mass considered in the reference case is 100 grams, exhibiting a maximum desorption capacity of 1.4 grams of hydrogen. In subfigure (a) of the plots, the temperature profile of the solid material is illustrated, indicating a swift rise from 300 K to 350 K, suggesting the effectiveness of the employed heat exchange method. Plots (a) and (b) feature lines representing the temperature and weight fraction of hydrogen across different sections of the hydride. Notably, the final section of the hydride at x = L initiates hydrogen desorption around the 400-second mark, although most of the desorption activity

occurs within the first 300 seconds, as evidenced by the purple dotted line. Comparative analysis reveals that the desorption time achieved in the reference case is significantly shorter than that reported in existing literature by authors such as Nasrallah, Chung, and Chandra [13], [23], [24]. This highlights the effectiveness of the proposed system design and operational parameters. Subfigures (c) and (d) show the thermal power and pumping power required by the system. The thermal power exhibits a peak at the beginning of the simulation, gradually decreasing as the hydrides attain higher temperatures until it eventually reaches zero. Despite the brief period of maximum power demand at the beginning of the simulation, the peak power required by the heat exchanger is noteworthy, considering the small dimensions of the reactor. However, this peak demand is short-lived. In contrast, the pumping power initially approaches its maximum value and then remains relatively constant throughout the entire simulation until the desorption process concludes. Subsequently, due to the increased pressure drop, there is a slight uptick in the pumping power. The pumping power remains low, attributed to the limited thickness of the bed and the omission of other pressure drops in the analysis. The primary energy consumption component in the reference case is thermal power, while even if pressure drop across a porous bed can escalate rapidly with increased thickness, the selection of a disk-shaped reactor with low thickness aims to mitigate pumping power requirements.

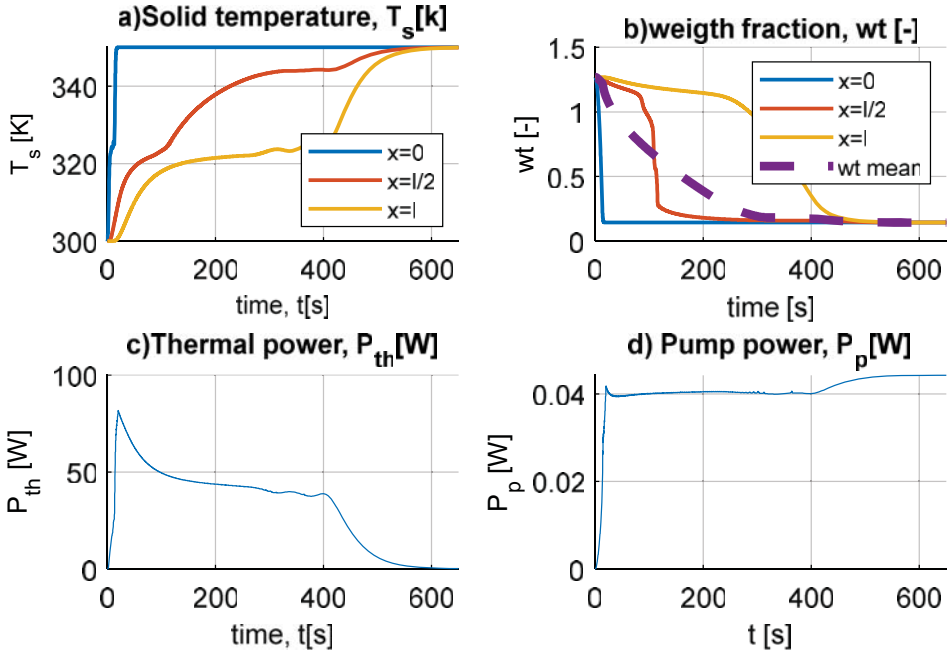

Figure 2: Results for the reference case with time, t, as a variable on the x axes. a) temperature of the metal hydride; b) weight fraction of hydrogen inside the hydride; c) Thermal power of the heat exchanger; d) pumping power of the fan.

3.2 Parametric analysis of geometry variables

Figure 3 shows the results for desorption time, mass, and the consumption of auxiliaries, with variations in the geometrical dimensions of the metal hydride reactor while keeping the porometry and thermodynamic variables constant for the desorption case. The chosen reactor shape aims to minimize pressure drop over the hydride while maximizing available surface area and volume. Desorption time and mass, depicted in charts (a) and (b) respectively, increase as the reactor dimensions rise, correlating with the amount of solid mass. Time to achieve a complete desorption of hydrogen from the hydride peaks at approximately 1400 seconds around a diameter of 100 mm and a length of 6 mm,

while desorbed mass approaches its maximum only for maximum diameter and length combinations. This suggests that hydrides capable of desorbing mass between 3 and 5 grams may not be optimal for minimizing desorption time. Regarding pumping power and energy and values remain low. This is attributed to the small length and moderate section of the reactor, resulting in minimal flow rate and pressure drop, average results being 50 l/min and 500 Pa. Consequently, pumping power and energy exert minimal impact. However, the peak power required, and energy consumption, rise notably with increased hydride length, indicating a significant increase in powder pressure drop. The thermal power is minimally impacted by the length of the hydrides but significantly influenced by the diameter, which also has a greater effect on the total volume. The variation observed is relatively low, ranging from 45 to 55 W. The peak in thermal power is sustained for only a limited duration during the process. The energy required for desorption falls within the range of 15 to 70 kJ. The combined thermal and electric energy needed for the absorption process accounts for approximately 8-9% of the total lower heating value of the desorbed hydrogen. This consumption level surpasses that associated with compressed hydrogen storage (3-4%) but falls short when compared to the energy consumption of liquid hydrogen storage methods (15-20 %) [25].

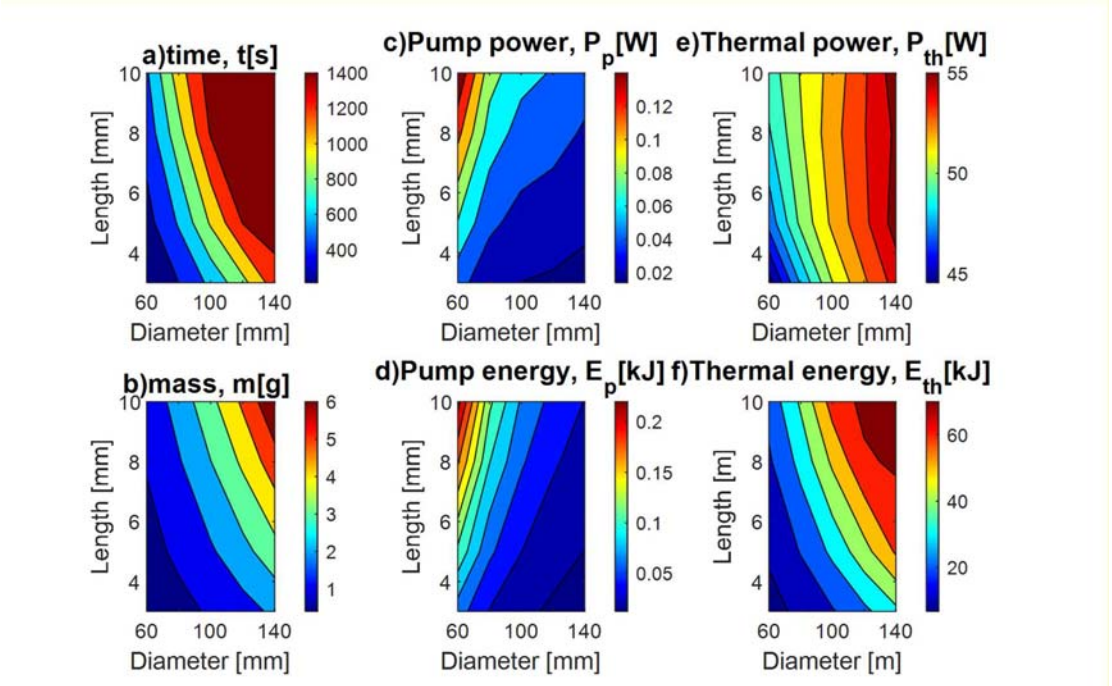

Figure 3: Results varying geometry variable length, L and diameter, D; a) time, t, to desorb all the hydrogen in the hydride; b) mass, m, of hydrogen desorbed in grams; c) pumping power, P_p; d) pumping energy, E_p; e) thermal power, P_{th} f) thermal energy, E_{th}

3.3 Parametric analysis of porometry variables

Figure 4 presents the same set of charts as before, this time exploring variations in porometry, specifically porosity of the bed and particle diameter, while maintaining constant reactor geometry and hydrogen gas inlet conditions. Desorption time and mass appear independent of particle diameter but heavily reliant on porosity. The impact of porosity on these parameters correlates with the amount of solid mass. Lower porosity results in more hydride mass within the same reactor volume, thereby increasing desorption time and maximum extractable mass. Regarding Figures c and d, the influence of porosity and particle diameter on pumping power and energy is minimal. However, a peak in both is observed at low porosity and particle diameter due to their combined effect on pressure drop. Lower

porosity and particle diameter reduce the permeability of the solid bed, leading to a rapid increase in pressure drop. Maintaining porosity above 0.4 and particle diameter above 50 microns is crucial to ensure reasonable pressure drops and flow rates along the reactor. While thermal power and thermal energy are minimally influenced by particle diameter, porosity emerges as the primary variable impacting results. This trend aligns with other cases, where the volume of solid mass remains the principal driver of outcomes.

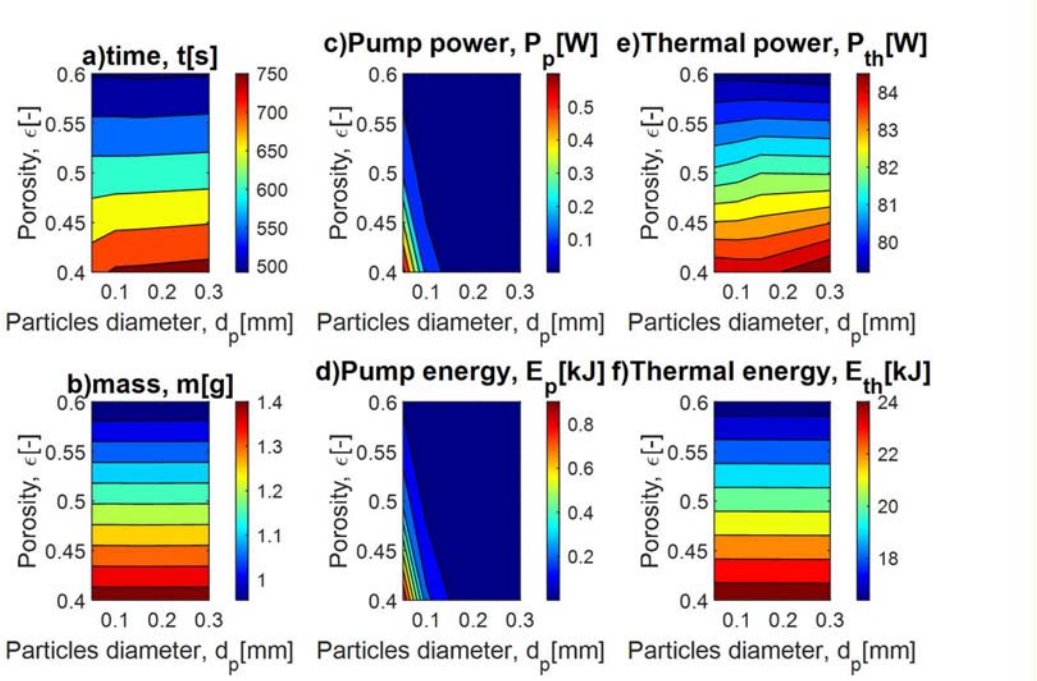

Figure 4: Results varying porometry variables porosity, epsilon,ϵ and particle diameters, d_p ; a) time, t, to desorb all the hydrogen in the hydride; b) mass, m, of hydrogen desorbed in grams; c) pumping power, P_p; d) pumping energy, E_p; e) thermal power, P_{th} f) thermal energy, E_{th}

3.4 Parametric analysis of thermodynamic variables

Figure 5 and Figure 6 present the results obtained varying the inlet temperature and pressure of the hydrogen gas at the beginning of the hydride as well as the mass flow rate of the hydrogen. Figure 5 shows the results with a fixed inlet mass flow rate of 0.05 g/s while in figure 6 it is considered to have double the amount of flow rate, 0.1 g/s. Starting from figure 5, the desorption time reduces significantly with the temperature, going from 1400s to 1000s from 30 to 60 degress of temperature difference. However, there is a peak in performances at low temperatures and high pressures, peak that does not happen at high pressure if the temperature rise. This behaviour is dependent on the fact that at high pressure at low temperature the desorption reaction reaches equilibrium at a weight fraction of the hydrogen that is higher than 0, this is clear if we consider also the chart b, where at high pressure and low temperature there is also a low desorbed mass. These trends can be seen in the same way but with higher magnitude in figure 6 a, where the desorption time goes as low as 500 seconds.

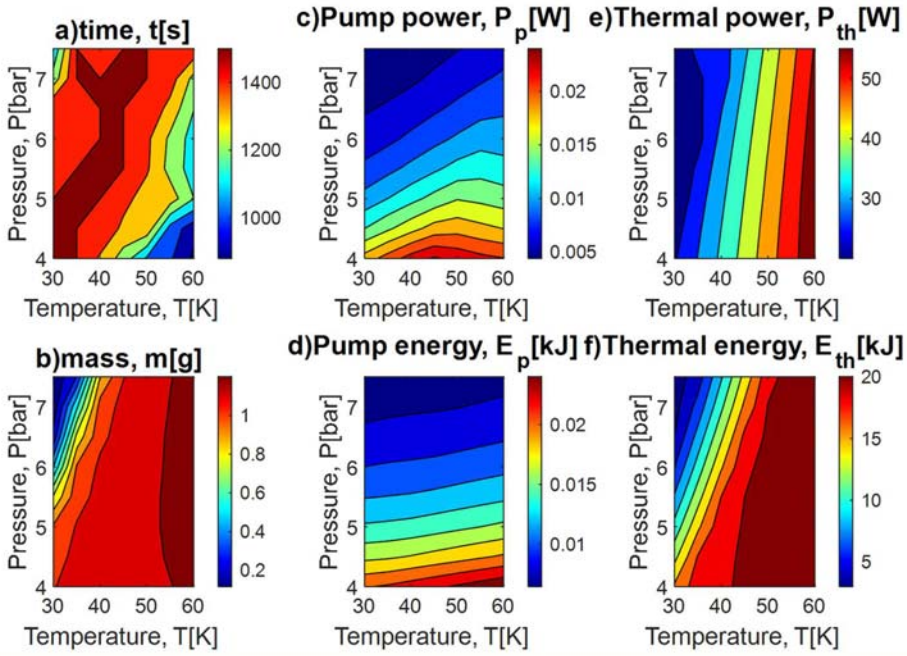

Figure 5: results varying temperature and pressure keeping the flow rate at 0.05 g/s. ; a) time, t, to desorb all the hydrogen in the hydride; b) mass, m, of hydrogen desorbed in grams; c) pumping power, P_p; d) pumping energy, E_p; e) thermal power, P_{th} f) thermal energy, E_{th}

For both the values of the flow rate the desorbed mass is a function mostly of the temperature difference given by the heat exchanger. The maximum amount of desorbed mass can be achieved at high temperatures and it is almost non dependant on the flow rate. The subfigures c and d show the pumping power and pumping energy with respect to temperature and pressure. The trends are similar, the energy and power are lower at high pressure and rise progressively with the pressure decrease and are slightly affected by the temperature increase. At high temperatures the pumping power and energy is slightly higher. The main difference between the figure 5 and 6 is in the order of magnitude. In figure 6 the pumping power is 3 times larger than the pumping power of figure 5 and the pumping energy is 5 times larger, while the flow rate doubles. The opposite situation can be seen from charts e and f for both figure 5 and 6. The thermal power and thermal energy are mostly dependent on the temperature, while slightly dependent on the pressure, with an increase at high temperatures. This is coherent with the kinetic models that describe the mechanism of desorption. It is noteworthy that the employed thermal management arrangement it is effective in rising the temperature of the hydride and sustain the reaction thought the process.

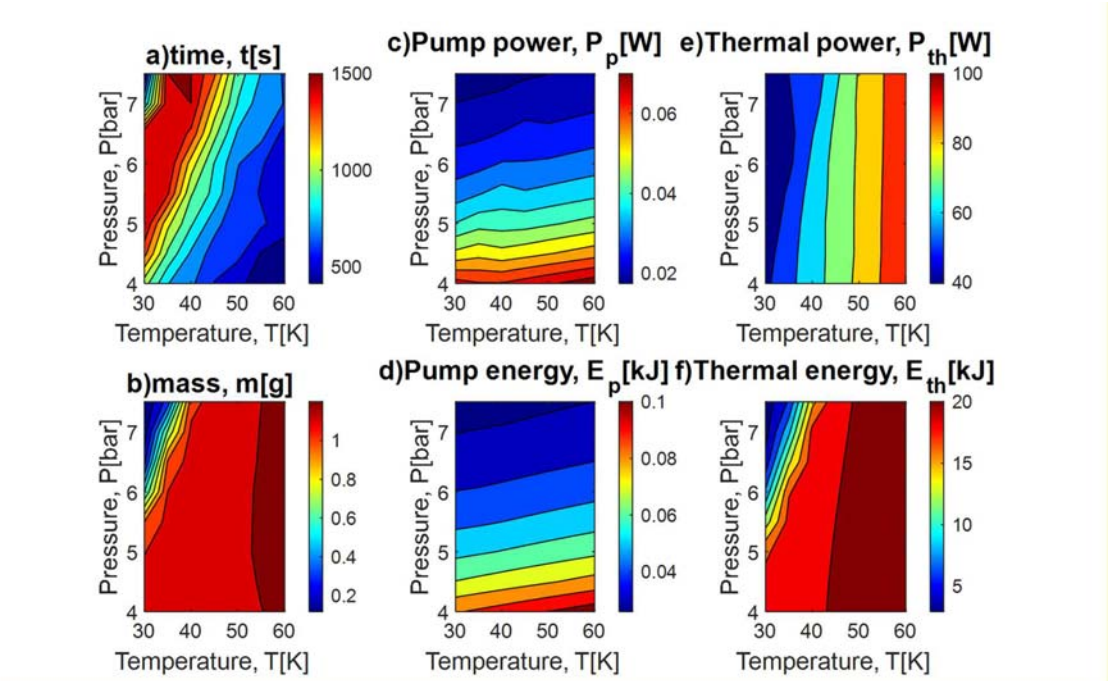

Figure 6: Results varying temperature and pressure keeping the flow rate at 0.1 g/s, double the amount with respect to figure 5; a) time, t, to desorb all the hydrogen in the hydride; b) mass, m, of hydrogen desorbed in grams; c) pumping power, P_p; d) pumping energy, E_p; e) thermal power, P_{th} f) thermal energy, E_{th}

The main difference between a flow rate of 0.05 g/s and 0.1 g/s is in the thermal power required that in the second case is twice the power, while the total amount of thermal energy to the hydride is constant with respect to the flow rate. The thermal energy being constant is reasonable with the fact that since the desorbed mass is the same it is required the same energy to sustain the reaction.

4 Conclusions

This study depicts a numerical model to simulate the performance of metal hydrides utilizing hydrogen as a direct fluid heat exchanger. The model, formulated as a system of partial differential equations, is solved using MATLAB ODE15s solver. It is applied to a case study involving a disk-type lanthanum nickel reactor, where hydrogen serves as the direct heat exchange fluid. The system performances are analyzed by varying several design parameters, including the length and diameter of the reactor, bed porosity, hydride particle diameter, pressure, temperature, and hydrogen mass flow rate at the reactor inlet. The main findings are as follows:

- Using hydrogen as a direct heat exchange fluid in a disk-type reactor with a length of 0.005 m and a diameter of 0.08 m facilitates rapid desorption, particularly with a porosity of 0.5 and a particle diameter of 100 microns. Complete desorption is achieved within 400 seconds, with the majority occurring before the 300-second mark. The required pumping power is consistently low due to minimal pressure drops and flow rates, while thermal power, although significant, is high only during a brief portion of the desorption process.
- The reactor geometry is crucial for achieving fast desorption and minimizing auxiliary energy consumption. The reactor volume primarily determines desorption time, desorbed mass, and the required thermal energy. The combined thermal and electric energy needed for the

absorption process constitutes approximately 8-9% of the total lower heating value of the desorbed hydrogen.

- Porosity has a greater impact on results compared to particle diameter. Higher porosity indicates more void spaces, leading to lower solid mass and, consequently, lower hydrogen content within a constant volume, reducing desorbed hydrogen from 1.4 to 1 gram. The occupied volume of solid mass significantly influences desorbed mass, time, and energy. Pumping power and energy are relatively unaffected by these parameters, remaining constant at 0.1 W and 0.2 kJ, respectively.
- Temperature, pressure, and flow rate clearly impact the results. The reaction is more efficient at high temperatures, low pressures, and high hydrogen recirculation rates, achieving 1 gram of desorbed hydrogen in under 500 seconds with an inlet hydrogen temperature of 360 K and total pressure of 3 bar. Pumping energy is lower at high pressure and low temperature, increasing from 0.015 to 0.08 kJ, with a fivefold rise in response to a doubled inlet flow rate. Thermal energy peaks at high temperatures and remains constant with respect to flow rate, with a maximum value of 20 kJ.

Based on the conclusions of this study, several possibilities for future improvement and expansion can be considered. Simulating the absorption process is necessary for a comprehensive understanding of the hydride working principle during hydrogen charging. The model can be adapted to simulate other types of hydrides by adjusting constants and hydride properties. Future analyses could focus on compounds less reliant on rare earth materials, such as high-temperature hydrides or complex hydrides. Finally, experimental analysis is essential to validate the model and confirm the consistency of the results.

Acknowledgements

The authors acknowledge “the PRIN: PROGETTI DI RICERCA DI RILEVANTE INTERESSE NAZIONALE – Bando 2020” Prot. 2020AA9N4M for the economic support.

References

[1] IEA, “The Future of Hydrogen.”
[2] K. C. Hoffman, J. J. Reilly, F. J. Salzano, C. H. Waide, R. H. Wiswall, and W. E. Winsche, “METAL HYDRIDE STORAGE FOR MOBILE STATIONARY APPLICATIONS-i,” Pergamon Press, 1976.
[3] G. Sandrock, “A panoramic overview of hydrogen storage alloys from a gas reaction point of view,” 1999.
[4] P. Modi and K. F. Aguey-Zinsou, “Room Temperature Metal Hydrides for Stationary and Heat Storage Applications: A Review,” *Frontiers in Energy Research*, vol. 9. Frontiers Media S.A., Apr. 09, 2021. doi: 10.3389/fenrg.2021.616115.
[5] B. Sakintuna, F. Lamari-Darkrim, and M. Hirscher, “Metal hydride materials for solid hydrogen storage: A review,” *International Journal of Hydrogen Energy*, vol. 32, no. 9. pp. 1121–1140, Jun. 2007. doi: 10.1016/j.ijhydene.2006.11.022.
[6] J. Bellosta von Colbe *et al.*, “Application of hydrides in hydrogen storage and compression: Achievements, outlook and perspectives,” *Int J Hydrogen Energy*, vol. 44, no. 15, pp. 7780–7808, Mar. 2019, doi: 10.1016/j.ijhydene.2019.01.104.
[7] A. Jemni and S. Ben Nasrallah, “STUDY OF TWO-DIMENSIONAL HEAT AND MASS TRANSFER DURING ABSORPTION IN A METAL-HYDROGEN REACTOR,” 1995.
[8] S. S. Mohammadshahi, E. M. A. Gray, and C. J. Webb, “A review of mathematical modelling of metal-hydride systems for hydrogen storage applications,” *International Journal of Hydrogen Energy*, vol. 41, no. 5. Elsevier Ltd, pp. 3470–3484, Feb. 09, 2016. doi: 10.1016/j.ijhydene.2015.12.079.

[9] Chibani Atef, Merouani Slimane, and Bougriou Cherif, "Chibani_et_al-2022-ThePerformanceOfHydrogenDesorptionFromAMetalHydrideWithHeatSupplyByAPhaseChangeMaterialIncorporatedInMetalFoamHeat&MassTransferAssessment," *J Energy Storage*, no. 51, 2022.

[10] S. A. Cetinkaya, T. Disli, G. Soyturk, O. Kizilkan, and C. O. Colpan, "A Review on Thermal Coupling of Metal Hydride Storage Tanks with Fuel Cells and Electrolyzers," *Energies*, vol. 16, no. 1. MDPI, Jan. 01, 2023. doi: 10.3390/en16010341.

[11] F. Laurencelle and J. Goyette, "Simulation of heat transfer in a metal hydride reactor with aluminium foam," *Int J Hydrogen Energy*, vol. 32, no. 14, pp. 2957–2964, Sep. 2007, doi: 10.1016/j.ijhydene.2006.12.007.

[12] S. Inoue, Y. Iba, and Y. Matsumura, "Drastic enhancement of effective thermal conductivity of a metal hydride packed bed by direct synthesis of single-walled carbon nanotubes," *Int J Hydrogen Energy*, vol. 37, no. 2, pp. 1836–1841, Jan. 2012, doi: 10.1016/j.ijhydene.2011.10.031.

[13] S. Chandra, P. Sharma, P. Muthukumar, and S. Sarma V Tatiparti, "Experimental hydrogen sorption study on a LaNi5-based 5 kg reactor with novel conical fins and water tubes and its numerical scale-up through a modular approach," *Int J Hydrogen Energy*, Dec. 2022, doi: 10.1016/j.ijhydene.2022.08.098.

[14] M. V. Lototskyy, I. Tolj, A. Parsons, F. Smith, C. Sita, and V. Linkov, "Performance of electric forklift with low-temperature polymer exchange membrane fuel cell power module and metal hydride hydrogen storage extension tank," *J Power Sources*, vol. 316, pp. 239–250, Jun. 2016, doi: 10.1016/j.jpowsour.2016.03.058.

[15] M. V. Lototskyy, I. Tolj, L. Pickering, C. Sita, F. Barbir, and V. Yartys, "The use of metal hydrides in fuel cell applications," *Progress in Natural Science: Materials International*, vol. 27, no. 1. Elsevier B.V., pp. 3–20, Feb. 01, 2017. doi: 10.1016/j.pnsc.2017.01.008.

[16] K. Yoshida, K. Kajiwara, H. Sugime, S. Noda, and N. Hanada, "Numerical simulation of heat supply and hydrogen desorption by hydrogen flow to porous MgH2 sheet," *Chemical Engineering Journal*, vol. 421, Oct. 2021, doi: 10.1016/j.cej.2021.129648.

[17] Y. Song *et al.*, "Fast Mg-based hydrogen storage with flow-through hydrogen as a cooling medium: A numerical study," *Int J Hydrogen Energy*, vol. 50, pp. 235–246, Jan. 2024, doi: 10.1016/j.ijhydene.2023.07.025.

[18] U. Mayer, M. Groll, and W. Supper, "HEAT AND MASS TRANSFER IN METAL HYDRIDE REACTION BEDS: EXPERIMENTAL AND THEORETICAL RESULTS*," 1987.

[19] S. Ben Nasrallah and A. Jemni, "HEAT AND MASS TRANSFER MODELS IN METAL-HYDROGEN REACTOR," 1996.

[20] F. Askri, "Study of two-dimensional and dynamic heat and mass transfer in a metal–hydrogen reactor," *Int J Hydrogen Energy*, vol. 28, no. 5, pp. 537–557, May 2003, doi: 10.1016/S0360-3199(02)00141-6.

[21] B. E. Logan, D. G. Jewett, R. G. Arnold, E. J. Bouwer, and C. R. O'Melia, "Clarification of Clean-Bed Filtration Models," *Journal of Environmental Engineering*, vol. 121, no. 12, pp. 869–873, Dec. 1995, doi: 10.1061/(asce)0733-9372(1995)121:12(869).

[22] F. Kuwahara, M. Shirota, and A. Nakayama, "A numerical study of interfacial convective heat transfer coe cient in two-energy equation model for convection in porous media," 2000, [Online]. Available: www.elsevier.com/locate/ijhmt

[23] A. Jemni and S. Ben Nasrallah, "STUDY OF TWO-DIMENSIONAL HEAT AND MASS TRANSFER DURING DESORPTION IN A METAL-HYDROGEN REACTOR," 1995.

[24] C. A. Chung, S. W. Yang, C. Y. Yang, C. W. Hsu, and P. Y. Chiu, "Experimental study on the hydrogen charge and discharge rates of metal hydride tanks using heat pipes to enhance heat transfer," *Appl Energy*, vol. 103, pp. 581–587, 2013, doi: 10.1016/j.apenergy.2012.10.024.

[25] A. Bauer, T. Mayer, M. Semmel, M. A. Guerrero Morales, and J. Wind, "Energetic evaluation of hydrogen refueling stations with liquid or gaseous stored hydrogen," *Int J Hydrogen Energy*, vol. 44, no. 13, pp. 6795–6812, Mar. 2019, doi: 10.1016/j.ijhydene.2019.01.087.